

MASTER

SLAC-PUB-2111
April 1978
(T/E)

CHARGED AND NEUTRAL CURRENT COUPLINGS OF QUARKS*
(As Seen By Neutrinos)

R. Michael Barnett

Stanford Linear Accelerator Center
Stanford University, Stanford, California 94305

Invited talk given at the 3rd International Conference at
Vanderbilt on New Results in High Energy Physics, March 6-8, 1978,
Nashville, Tennessee

NOTICE

This report was prepared as an account of work sponsored by the United States Government. Neither the United States nor the United States Energy Research and Development Administration, or any of their contractors, or their employees, makes any warranty, express or implied, or assumes any legal liability or responsibility for the accuracy, completeness, or usefulness of any information, apparatus, product or process disclosed, or represents that its use would not infringe privately owned rights.

*Research supported by the Department of Energy

There is now considerable information about the couplings of quarks to gauge bosons in theories of the weak and electromagnetic interactions. Much has been learned about charged-current couplings from the energy dependence of neutrino cross-sections and of y distributions, and also from the lack of t and b quark production in neutrino scattering. Knowledge of neutral-current couplings has also come mainly from neutrino experiments. In this talk I will first discuss aspects of charged-current scattering including the question of whether the cross-sections are "anomalous" in any sense and the subject of limits on the production of new heavy quarks. In the second part, I will discuss a new, unique determination of neutral-current couplings, using data from deep-inelastic and elastic neutrino scatterings and from neutrino-induced exclusive and inclusive pion production.

The Weinberg-Salam (WS) theory¹ of weak and electromagnetic interactions with the Glashow-Iliopoulos-Maiani (GIM) quark structure² has been a remarkable phenomenological success when compared with all other weak interaction models. It is worthwhile, therefore, to discuss charged-current couplings in that context before in more general contexts. The WS-GIM model has the couplings:

$$\begin{pmatrix} u \\ d \end{pmatrix}_L \begin{pmatrix} c \\ s' \end{pmatrix}_L \begin{pmatrix} t \\ b' \end{pmatrix}_L$$

where the primes indicate that the weak interaction eigenstates (d' , s' , b') do not coincide with the mass eigenstates (d , s , b). This mixing among the quark states is indicated with the weak coupling matrix³:

$$\begin{matrix} & \begin{matrix} u & s & b \end{matrix} \\ \begin{matrix} u \\ c \\ t \end{matrix} & \begin{pmatrix} c_c & -s_c c_2 & -s_c s_2 \\ s_c c_1 & c_c c_1 c_2 - s_1 s_2 e^{i\theta} & c_c c_1 s_2 + s_1 c_2 e^{i\theta} \\ s_c s_1 & c_c s_1 c_2 + c_1 s_2 e^{i\theta} & c_c s_1 s_2 - c_1 c_2 e^{i\theta} \end{pmatrix} \end{matrix}$$

where $c_1 \equiv \cos \theta_c$, $s_1 \equiv \sin \theta_c$, etc. and the rows and columns correspond to the quarks indicated. In the discussion which follows, I use the notation $u_{ij} = U_{ij}(W \gamma_5) d_j$.

J. Ellis et al.⁴ have noted that the universality of quark and lepton couplings requires (in the WS-GIM model) that the ratio of coupling constants squared ($|U_{ij}|^2$ to $|U_{ij}|$ (which is $\tan^2 \theta_c \sin^2 \theta_c$)) be less than 0.003. Since the ratio of U_{ij} to U_{ij} is 0.05, one finds that $\sin^2 \theta_c = \tan^2 \theta_c < 0.1$ and that in this six-quark model θ_c is equal to the usual Cabibbo angle ($\theta_c = 13^\circ$).

The determination of limits on θ_c is more complicated. J. Ellis et al.⁵ have also noted that an estimate can be obtained following a procedure analogous to that of Gaillard and Lee⁶ for a four-quark model. These latter authors used the K_L - K_S mass difference to estimate the charmed-quark mass (given the Cabibbo angle). When this procedure is extended to the six-quark model, one finds that the results depend on the accuracy of the Gaillard-Lee estimate of the K_L^0 - K_S^0 transition amplitude (they suggested that their

estimate of the amplitude was good within an order of magnitude). If f is defined as the multiplicative deviation from their estimate, then the ratio of coupling constants squared for $\bar{t}d_L$ to $\bar{u}d_L$ ($\tan^2\theta_c \sin^2\theta_1$) can be found as a function of f and the mass of the t quark (with $m_c = 1.5$ GeV):

	$f=1$	$f=2$	$f=5$
$m_t = 5$ GeV	0	0.012	0.031
$m_t = 15$ GeV	0	0.0035	0.013

While these limits are not as severe as for $\bar{u}b_L$, the coupling $\bar{t}d_L$ is nonetheless quite small.

One can say that $\sin^2\theta_1 \leq 0.4$ even for a 5 GeV quark. Therefore, the coupling $\bar{t}d_L$ is always much smaller than $\bar{c}s_L$, and the coupling $\bar{t}b_L$ is large. Since the signs of $\sin\theta_1$ and $\sin\theta_2$ are not known, one cannot make definitive statements about the relative magnitudes of $\bar{t}s_L$ to $\bar{t}d_L$ or of $\bar{c}b_L$ to $\bar{u}b_L$. However, for most (but not all) angles, the coupling constants squared for $\bar{t}s_L$ and $\bar{c}b_L$ are much larger than those for $\bar{t}d_L$ and $\bar{u}b_L$, respectively.

In summary, for the WS-GIM model, the t quark should couple dominantly to the b quark, with (in most cases) a secondary coupling to s quarks and with a relatively small coupling to d quarks. The b quark, if it is lighter than the t quark, is likely to decay into c quarks. The b quark should have a very small coupling to u quarks.

In order to consider more general limits on charged-current couplings (outside the context of the WS-GIM model), one can study the energy dependence of σ_{tot} and $\langle y \rangle$ in neutrino scattering, $\nu_\mu N \rightarrow \nu + X$ (where $y \equiv (E_\nu - E_\mu)/E_\nu$). The applicability of limits from neutrino experiments is restricted to couplings via those gauge bosons which also couple to ν_μ ; in most models, this means the usual W boson. The requirement used in determining limits is that consistency with all available data be obtained. Some care must be given, since each experiment has different cuts, efficiencies and corrections to the data. All curves shown below were calculated in the context of QCD (i.e. - they contain scaling violations).

In Fig. 1 the data from neutrino scattering for the average value of y versus energy are shown. The line is the prediction (with QCD corrections included) for the WS-GIM model. The CERN-Dortmund-

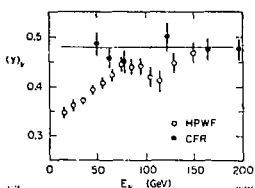


Fig. 1. The average value of y in deep-inelastic neutrino scattering versus energy. The line is the QCD prediction for the standard four-quark model. The data are from Refs. 7 and 8.

Heidelberg-Saclay (CDHS) data⁶ which are not shown have no energy dependence consistent with the Cal Tech-Fermilab-Rockefeller (CFR) data.⁷ The Harvard-Pennsylvania-Wisconsin-Fermilab (HPWF) data⁸ contain efficiencies and cuts which reduce $\langle y \rangle$ at low energies. It is clear that the WS-GIM model is consistent with the data. For neutrinos, $\langle y \rangle$ does not set significant limits on any couplings.

The cross-section for charged-current neutrino scattering⁹ is shown in Fig. 2. The lowest solid curve is the prediction of the WS-GIM model. The three solid curves show the effect of a $\bar{t}d_L$ coupling equal in magnitude to $\bar{u}d_L$ for $m_t = 5, 7,$ and 9 GeV (from top). One can say roughly that $m_t \gtrsim 8 \text{ GeV}$. The dotted curve is the result of a $\bar{t}d_R$ coupling for a 5 GeV t quark. In this case there is not a strict limit, and one can conclude only that $m_t \gtrsim 6 \text{ GeV}$. Of course, one learns more about $\bar{t}d_R$ couplings from neutral-current interaction as is discussed later.

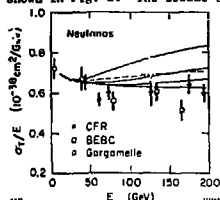


Fig. 2. The total charged-current cross-section for neutrino scattering vs. energy. The solid curves are the QCD predictions for the standard four-quark model with (from bottom to top): 1) no $\bar{t}d_L$, 2) $\bar{t}d_L$ added and $m_t = 9 \text{ GeV}$, 3) $m_t = 7 \text{ GeV}$. The dotted curve has $\bar{t}d_R$ added with $m_t = 5 \text{ GeV}$. The data are from Ref. 9.

The limits obtained for $\bar{u}b_L$ couplings are not quite as strict as for $\bar{t}d_L$. As long as $m_b > 7 \text{ GeV}$, the coupling could be as strong as for $\bar{u}d_L$. If $m_b = 5 \text{ GeV}$, then the coupling squared for $\bar{u}b_L$ can be 0.7 or less of that for $\bar{u}d_L$. Therefore, a substantial admixture of $\bar{u}b_L$ is allowed (although much stronger limits were found for the WS-GIM model earlier).

To study the possibility of a $\bar{u}b_R$ coupling, one can examine σ_{tot} and $\langle y \rangle$ in antineutrino scattering which are shown⁶⁻⁹ in Figs. 3 and 4. Clearly there is absolutely no need for any $\bar{u}b_R$ coupling. Any energy dependence present in the data is probably just that expected from scaling violations resulting from QCD corrections.¹⁰ Since the data from different collaborations have different cuts, efficiencies and corrections, some experimentalists prefer to use the variable B which is determined by fitting to

$$\frac{d^2\sigma^{\bar{\nu},\bar{\nu}}}{dxdy} = \frac{G^2 M_E}{\pi} F_2(x) \left[\frac{(1+B)}{2} + \frac{(1-B)}{2} (1-y)^2 \right]$$

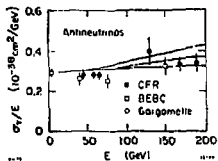


Fig. 3. The total charged-current cross-section for antineutrino scattering vs. energy. The solid curves are the QCD predictions for the standard four-quark model with (from bottom to top): 1) no $\bar{u}g_R$, 2) $\bar{u}g_R$ added and $m_b=9 \text{ GeV}$, 3) $m_b=7 \text{ GeV}$. The data are from Ref. 9.

where

$$B = -xF_3(x)/F_2(x).$$

Fig. 5 shows the data⁵⁻⁹ and the QCD predictions without and with a coupling $\bar{u}g_R$ (for $m_b = 7, 9, 11 \text{ GeV}$). It is evident from this figure (and from Figs. 3 and 4) that $m_b \geq 11 \text{ GeV}$ if $\bar{u}g_R$ has the same strength as $\bar{d}g_L$. Also shown in Fig. 5 are the curves for $\bar{u}g_L$ which lead to the limits discussed earlier. If one examines the effects of $m_b = 5 \text{ GeV}$ (motivated by the existence of $T(9.4)$), then the ratio of couplings squared for $\bar{u}g_R$ to $\bar{d}g_L$ must be 0.1 or less, as seen in Fig. 6.

These are very strict limits. While the results given here (and shown in the figures) include the scaling violations of QCD, little change in the limits results even if all scaling violation is ignored. The data shown in Figs. 3-5 indicate (for each experiment) that there is very little variation with energy above $E = 50 \text{ GeV}$; this result is consistent with the expectations from QCD. However, below 50 GeV the situation is not at all clear. Leaving aside the dispute over the existence of a "low- y anomaly", the question of energy dependence at "low" energies is very interesting. An important test of QCD would be obtained with a careful measurement by a single experiment of the energy dependence of $\langle y \rangle$ and σ_{tot} between 10 and 50 GeV. Of course, another excellent test is the q^2 dependence of the structure function $F_2(x)$ or, similarly, the E dependence of $\langle x \rangle$. At present, QCD is the only theory of the strong interactions, and it is vital, therefore, to test its predictions.

The question of the possible existence of $\bar{u}g_R$ or $\bar{d}g_R$ couplings can be addressed from a completely different perspective. In gauge theories of the weak and electromagnetic interactions, the charged-

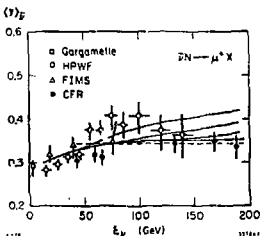


Fig. 4. The average value of y in deep-inelastic antineutrino scattering vs. energy. The solid curves are the QCD predictions for the standard four-quark model with (from bottom to top): 1) no $\bar{u}g_R$, 2) $\bar{u}g_R$ added and $m_b=11 \text{ GeV}$, 3) $m_b=9 \text{ GeV}$, 4) $m_b=7 \text{ GeV}$. The dashed line represents the values for CDHS data reported by J. Steinberger.⁹ The data are from Ref. 9.

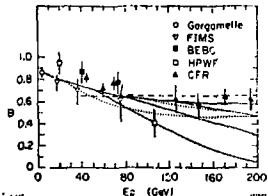


Fig. 5. The B parameter for anti-neutrinos vs. energy. The solid curves are the QCD predictions for the standard four-quark model with (from top to bottom): 1) no $\bar{u}b_R$, 2) $\bar{u}b_R$ added and $m_b=11$ GeV, 3) $m_b=9$ GeV, 4) $m_b=7$ GeV. The two dotted curves have $\bar{u}d_L$ added with (from top to bottom) $m_b=9$ GeV and $m_b=5$ GeV. The dashed line represents the value for CDHS data reported by J. Steinberger.⁹ The data are from Refs. 6-9.

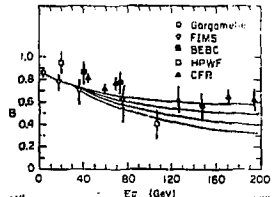


Fig. 6. The B parameter for anti-neutrinos vs. energy. The solid curves are the QCD predictions for the standard four-quark model with (from top to bottom): 1) no $\bar{u}b_R$, 2) $\bar{u}b_R$ added, $m_b=5$ GeV, and couplings squared 0.1 of $\bar{u}d_L$, 3) 0.2 of $\bar{u}d_L$, 0.3 of $\bar{u}d_L$. The data are from Refs. 6-9.

current and neutral-current interactions are intimately related. For example, in $SU(2) \times U(1)$ models,¹ the weak neutral currents can be obtained by adding a term found by an isospin rotation of the charged currents to a term proportional to the electromagnetic current.

Larry Abbott and I have recently completed an analysis¹¹ of neutral-current couplings. Our analysis is independent of models, but the conclusions are, of course, applicable to any model. As will be shown, we have obtained a unique determination of the neutral-current couplings of u and d quarks which shows that in $SU(2) \times U(1)$ models, there can be no $\bar{d}d_R$ or $\bar{u}b_R$ couplings.

Askmun: a V,A structure and starting with the effective neutral-current Lagrangian:

$$\mathcal{L} = \frac{G}{\sqrt{2}} \bar{v} \gamma_\mu (1+\gamma_5) v \left[u_L \bar{u} \gamma_\mu (1+\gamma_5) u + u_R \bar{u} \gamma_\mu (i-\gamma_5) u \right. \\ \left. + d_L \bar{d} \gamma_\mu (1+\gamma_5) d + d_R \bar{d} \gamma_\mu (1-\gamma_5) d \right] ,$$

the allowed values of the coefficients u_L , u_R , d_L , and d_R were determined from four types of neutrino experiments. There is always an ambiguity in the overall sign of the four coefficients (couplings); we chose a sign convention by requiring u_L to always be positive.

The first input is data for deep-inelastic scattering ($vN \rightarrow vX$). We chose to use CDHS data¹² since it is at high energy ($\langle E \rangle \approx 100$ GeV) and has small error bars. These data give limits on the values of $u_L^2 + d_L^2$ and $u_R^2 + d_R^2$. When plotted on the u_L - d_L and u_R - d_R planes,

the regions allowed at the 90% confidence level are, therefore, annuli as shown in Fig. 7.

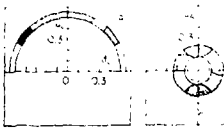


Fig. 7. The left (a) and right (b) coupling planes. Annular regions are allowed by deep-inelastic data. The region shaded with lines is allowed by deep-inelastic, elastic and exclusive-pion data. The regions shaded with dots are allowed by deep-inelastic and inclusive-pion data.

Since the radii are well-determined by the deep-inelastic data, it is useful in analyzing other data to plot the allowed values of the angles Θ_L and Θ_R which are defined as

$$\Theta_L = \arctan (v_L/d_L)$$

$$\Theta_R = \arctan (v_R/d_R)$$

This plot has the advantage of showing correlations between the left and right planes which are not evident in Fig. 7.

The next input is data for elastic neutrino-proton scattering ($v_p + v_p$). New data¹³ from the HPW collaboration for both neutrinos and antineutrinos has been reported at this conference and is used for this analysis. Significant portions of the possible angular regions are eliminated by this data. The allowed region (at the 90% confidence level) is contained within the dotted line in Fig. 8.

A crucial new input into this analysis is data for exclusive pion production¹⁴ for which six channels are available now:

$$\begin{aligned} v_p + v_p \pi^0 &\rightarrow \bar{n}N + \bar{\nu}N\pi^0 \\ v_n + v_n \pi^0 &\rightarrow \bar{n}n + \bar{\nu}p\pi^0 \\ v_p + v_n \pi^+ & \\ v_n + v_p \pi^- & \end{aligned}$$

To analyze these data, the detailed model of Adler¹⁵ was used. This model includes non-resonant production, incorporates excitation of the $\Delta(1232)$ resonance, and satisfies current algebra constraints. Because we ignore resonances with mass above 1.4 GeV and use soft-pion theorems, we must require that the invariant mass of the pion-nucleon system (ω) be less than 1.4 GeV. The data are not available with this cut (and cannot be obtained when a neutron is in the final state). Fortunately most of the cross-section is below $\omega = 1.4$ GeV, and indications are that application of the cut would strengthen our conclusions. Since we consider only neutral to charged current ratios, the effect of the cut is minimized. Since there is some uncertainty in the model used for analysis, the allowed region is defined as that region within a factor of two of the data (about 3 standard deviations). Application of the limits from these data reduced the allowed region to that shown by shading with lines in both Figs. 7 and 8. In Fig. 8 for $\Theta_L = 135^\circ$, any value of Θ_R was allowed by the elastic data, but now with the exclusive pion data the limits are greatly improved.

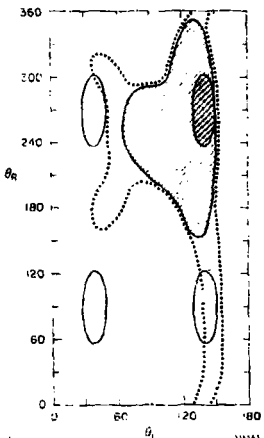


Fig. 8. Allowed angles for specific radii. The dotted curve indicates the area allowed by elastic data. The region shaded with lines is allowed by elastic and exclusive-pion data. The elliptical regions are allowed by inclusive-pion data. The area shaded with dots is the only region allowed by all data.

is shown on the right plane with a similar line, whereas for other $SU(2) \times U(1)$ models¹⁸⁻²⁰ (A, B and C) only the point corresponding to $\sin^2 \theta_W = 0.3$ (determined from the left plane) is shown on the right plane. Note that on both planes the WS model agrees with all data for $\sin^2 \theta_W$ between 0.22 and 0.30. In fact it is only for the m_2/m_W ratio found from the minimal Higgs boson structure¹ that agreement is obtained. This is a remarkable result.

For all other $SU(2) \times U(1)$ models, the predictions are far from the allowed region for any value of m_2/m_W . Those models are unequivocably ruled out. Also shown in Fig. 9 are the predictions of two

A final input is data for inclusive pion production¹⁶ ($\nu N \rightarrow \nu n X$). The analysis¹⁷ of these data requires significant parton-model assumptions; in particular, it is assumed that pions produced in the current (W -boson) fragmentation region are decay products of the struck quarks. The ratios of π^+ to π^- production for $0.3 < z < 0.7$ where $z = E_\pi/E_{\text{hadron}}$ were measured. The data were taken at low energies where one could question parton-model assumptions. However, our determination of neutral-current couplings is unique even without these data; its inclusion serves only to further reduce the one allowed region. In Figs. 7 and 8 the final allowed region (at the 90% confidence level) is shown by shading with both lines and dots.

This allowed region corresponds to the couplings

$$u_L = 0.33 \pm 0.07 \quad u_R = -0.18 \pm 0.06 \\ d_L = -0.40 \pm 0.07 \quad d_R = 0.0 \pm 0.11$$

where the errors are 90% confidence limits and an overall sign convention has been assumed.

Our results are compared with the predictions of various models in Fig. 9. $SU(2) \times U(1)$ models¹ all have the same prediction for the left plane, which is shown with a line indicating the results for different values of $\sin^2 \theta_W$. The WS model^{1,2}

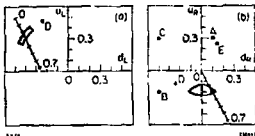


Fig. 9. Various gauge models compared with the allowed coupling constant region. The line marks the WS model for values of $\sin^2 \theta_W$ from 0.0 to 0.7. A, B and C indicate $SU(2) \times U(1)$ with A) a $\bar{u}g$ coupling¹⁸, B) a $\bar{d}g$ coupling¹⁹ and C) both couplings²⁰ (vector model). D and E indicate $SU(3) \times U(1)$ models with: D) u in a right-handed singlet²¹ and E) u in a right-handed triplet.²² For A, B, C and E, u_L and d_L lie within the shaded region.

Although neutrino experiments are very difficult, they provide powerful tools for analyzing the structure of the weak interactions. In the last few years, there has been enormous progress in determining the couplings of both charged and neutral currents of u and d quarks. In the future we can expect to learn more about the couplings of other quarks and of the leptons.

I would like to acknowledge contributions to this work from S. Adler, J. Bjorken, F. Gilman, A. Mann, C. Matteuzzi, Y. J. Ng, J. Strait, L. Sulak and especially Larry Abbott and François Martin.

REFERENCES

1. S. Weinberg, Phys. Rev. Lett. 19, 1264 (1967); A. Salam, in Elementary Particle Physics: Relativistic Groups and Analyticity, edited by N. Svartholm (Almqvist and Wiksell, Stockholm, 1968), p. 367.
2. S.L. Glashow, J. Iliopoulos and L. Maiani, Phys. Rev. D2, 1285 (1970).
3. M. Kobayashi and K. Maskawa, Prog. Theor. Phys. 49, 652 (1973).
4. J. Ellis et al., Nucl. Phys. B131, 285 (1977); J. Ellis, M.K. Gaillard, and D.V. Nanopoulos, Nucl. Phys. B132, 213 (1976).
5. M.K. Gaillard and B.W. Lee, Phys. Rev. D10, 897 (1974).
6. M. Holder et al., Phys. Rev. Lett. 39, 433 (1977).
7. F. Sciulli et al., in Proc. 1977 Int. Symposium on Lepton and Photon Interactions at High Energies, edited by F. Gutschrod (DESY, Hamburg, 1977), p. 239.

8. A. Benvenuti et al., Phys. Rev. Lett. 36, 1478.
9. B.C. Barish et al., (CFR), Phys. Rev. Lett. 39, 1595 (1977);
A. Benvenuti et al., (HPWT), Phys. Rev. Lett. 37, 189 (1976);
J.P. Berge et al., (FIMS), Phys. Rev. Lett. 39, 382 (1977);
P.C. Bosetti et al., (BEDC), Phys. Lett. 70B, 273 (1977),
K. Kleinknecht (CDHS), in Proc. 1977 Int. Symposium on Lepton and Photon Interactions at High Energies, edited by F. Gutbrod (DESY, Hamburg, 1977) p. 271; J. Steinberger, invited talk at the 1977 Irvine Conference.
10. G. Altarelli, G. Parisi, and R. Petronzio, Phys. Rev. Lett. 63B, 183 (1976); G. Altarelli and G. Parisi, Nucl. Phys. B126, 298 (1977); M. Barnett, H. Georgi and H.D. Politzer, Phys. Rev. Lett. 37, 1313 (1976); J. Kaplan and F. Martin, Nucl. Phys. B115, 333 (1977); M. Barnett and F. Martin, Phys. Rev. D10, 2765 (1977); V.I. Zakharov, in Proc. of the XVII Int. Conf. on High Energy Physics, Tbilisi, July 1976, edited by N.N. Bogoliubov et al. (Joint Institute for Nuclear Research, Dubna, 1977) Vol. II, p. B69; A. Zee, F. Wilczek and S.B. Treiman, Phys. Rev. D10, 2881 (1974); A.J. Buras and K.J.F. Gaemers, Phys. Lett. 71B, 106 (1977); A.J. Buras, Nucl. Phys. B125, 125 (1977); A.J. Buras et al., Nucl. Phys. B131, 308 (1977); G.C. Fox, Caltech Report CALT-68-619 (1977).
11. L.F. Abbott and R.M. Barnett, report SLAC-PUB-2097 (1978).
12. M. Holder et al., Phys. Lett. 72B, 254 (1977); see also J. Blietnick et al., Nucl. Phys. B118, 218 (1977); A. Benvenuti et al., Phys. Rev. Lett. 37, 1039 (1976); B.C. Barish et al., Caltech report no. CALT-68-601 (1977).
13. J. Strait, Harvard University Ph.D. thesis (1978), W. Kozanecki, Harvard University Ph.D. thesis (1978), and D. Cline et al., Phys. Rev. Lett. 37, 252 and 648 (1976); see also W. Lee et al., Phys. Rev. Lett. 37, 186 (1976); M. Pohl et al., report no. CERN/EP/PHYS 77-53 (1977).
14. W. Krenz et al., report no. CERN/EP/PHYS 77-50 (1977); O. Erriques et al., CERN report (1978); see also S.J. Barish et al., Phys. Rev. Lett. 33, 448 (1974); W. Lee et al., Phys. Rev. Lett. 38, 202 (1977).
15. S.L. Adler, Ann. Phys. 50, 189 (1968) and Phys. Rev. D12, 2644 (1975); see also S.L. Adler et al., Phys. Rev. D12, 3501 (1975).
16. H. Kluttig et al., Phys. Lett. 71B, 446 (1977).
17. L.M. Schul, Phys. Lett. 71B, 99 (1977); P.Q. Hung, Phys. Lett. 69B, 216 (1977); P. Scherbach, Nucl. Phys. B82, 155 (1974).
18. M. Barnett, Phys. Rev. Lett. 34, 41 (1975), Phys. Rev. D11, 3246 (1975); P. Fayet, Nucl. Phys. B78, 14 (1974); F. Gürsey and P. Sikivie, Phys. Rev. Lett. 36, 775 (1976); P. Ramond, Nucl. Phys. B110, 214 (1976).
19. M. Barnett, Phys. Rev. D13, 671 (1976).
20. A. De Rújula et al., Phys. Rev. D12, 3589 (1975); F.A. Wilczek et al., Phys. Rev. D12, 2768 (1975); H. Fritzsch et al., Phys. Lett. 59B, 256 (1975); S. Pakvasa et al., Phys. Rev. Lett. 35, 702 (1975).
21. G. Segre and J. Weyers, Phys. Lett. 65B, 243 (1976); B.W. Lee and S. Weinberg, Phys. Rev. Lett. 38, 1237 (1977); B.W. Lee and

R. Shrock, report no. Fermilab-PUB-77/48-THY.

- 22. M. Barnett and L.N. Chang, Phys. Lett. 72B, 233 (1977); M. Barnett et al., Phys. Rev. D (to be published); P. Langacker and G. Segre, Phys. Rev. Lett. 39, 259 (1977).
- 23. J. Pati and A. Salam, Phys. Rev. D10, 275 (1974); H. Fritzsch and P. Minkowski, Nucl. Phys. B103, 61 (1976); R.N. Mohapatra and D.P. Sidhu, Phys. Rev. Lett. 38, 667 (1977); A. De Rujula, H. Georgi and S.L. Glashow, Annals Phys. 109, 242 and 258 (1977).
- 24. H. Georgi and S. Weinberg, Phys. Rev. D17, 275 (1978).